Coevolutionary patterning of teeth and taste buds

Ryan F. Bloomquist[a,b,1], Nicholas F. Parnell[a], Kristine A. Phillips[a], Teresa E. Fowler[a], Tian Y. Yu[c], Paul T. Sharpe[c], and J. Todd Streelman[a,1]

[a]School of Biology and Institute for Bioengineering and Bioscience, Georgia Institute of Technology, Atlanta, GA 30332; [b]College of Dental Medicine, Georgia Regents University, Augusta, GA 30912; and [c]Department of Craniofacial Development and Stem Cell Biology, Dental Institute, King's College London, London WC2R 2LS, United Kingdom

Edited by Neil H. Shubin, University of Chicago, Chicago, IL, and approved September 16, 2015 (received for review July 22, 2015)

Teeth and taste buds are iteratively patterned structures that line the oro-pharynx of vertebrates. Biologists do not fully understand how teeth and taste buds develop from undifferentiated epithelium or how variation in organ density is regulated. These organs are typically studied independently because of their separate anatomical location in mammals: teeth on the jaw margin and taste buds on the tongue. However, in many aquatic animals like bony fishes, teeth and taste buds are colocalized one next to the other. Using genetic mapping in cichlid fishes, we identified shared loci controlling a positive correlation between tooth and taste bud densities. Genome intervals contained candidate genes expressed in tooth and taste bud fields. *sfrp5* and *bmper*, notable for roles in Wingless (Wnt) and bone morphogenetic protein (BMP) signaling, were differentially expressed across cichlid species with divergent tooth and taste bud density, and were expressed in the development of both organs in mice. Synexpression analysis and chemical manipulation of Wnt, BMP, and Hedgehog (Hh) pathways suggest that a common cichlid oral lamina is competent to form teeth or taste buds. Wnt signaling couples tooth and taste bud density and BMP and Hh mediate distinct organ identity. Synthesizing data from fish and mouse, we suggest that the Wnt-BMP-Hh regulatory hierarchy that configures teeth and taste buds on mammalian jaws and tongues may be an evolutionary remnant inherited from ancestors wherein these organs were copatterned from common epithelium.

quantitative trait loci | tooth/taste bud development | placode patterning | bipotency | plasticity

Hughes and Chuong (1) called the mammalian oral cavity a "mouthful of epithelial-mesenchymal interactions" because the same precursor epithelium must ultimately differentiate to form teeth in one row on the oral jaw margin, taste buds, and filiform papillae on the tongue, and salivary glands in precise locations. Developmental biologists have worked for decades to understand how this oral epithelium is properly fated to form such a diversity of structures. Although progress has been made to discover the molecules and pathways responsible for individual organ identity (2), we know much less about the genetics and development of tooth and taste bud patterning (i.e., the spacing, organization, and density of organs), and almost nothing about adaptive variation in dental and taste bud density across populations and species.

Because placode-derived structures, such as teeth and taste buds, tend to be located in different regions of the integument or the gastrointestinal tract to engage a particular function, they are studied independently. However, commonalities are apparent in the patterning of these appendages. Hair, feathers, glands, teeth, taste buds, and intestinal crypt villi are similarly induced under the direction of epithelial and mesenchymal interactions. Similar reaction-diffusion models have been proposed to control the size and spacing of manifold placode-derived organs (3), such as hair (4), feathers (5), and teeth (6). Activators and inhibitors in the bone morphogenetic protein (BMP), fibroblast growth factor (FGF), Hedgehog (Hh), and Wingless (Wnt) pathways execute the pattern. Genetic abnormalities in these pathways often lead to syndromic human diseases, such as Gardner's syndrome, Gorlin syndrome, and ectodermal dysplasia, which affect multiple appendages (7). Feedback loops have been independently identified wherein Wnt drives the initiation of dental (8) or taste (9) placodes. Wnt/β-catenin acts upstream of BMP and Hh signaling (10, 11), which in turn may regulate Wnt and organ identity (5–10).

Mammals typically possess a single row of teeth on the oral jaw and a distinct taste papillae-bearing tongue and posterior palate. In contrast, many vertebrate dentitions are found in multiple rows on multiple bony or cartilaginous structures throughout the oro-pharynx. Taste buds often colocalize with teeth at these sites as both organs are regenerated, with pattern fidelity, throughout the lifetime of an individual. Teeth and taste buds may share an evolutionary origin and deep molecular homology (12). There is tremendous variation in tooth and taste bud numbers among vertebrates. Among closely related species, this variation likely has ecological relevance (13). For example, in Lake Malawi cichlids, planktivores typically possess a small number of widely spaced teeth (14) with reduced taste bud counts on the oral jaws. Alternatively, the oral jaws of algivores are packed with hundreds to thousands of teeth and taste buds at higher density (*SI Appendix*, Fig. S1). We sought to understand the genetic and developmental underpinnings of covariation in tooth and taste bud density in Lake Malawi cichlids, in particular: (*i*) how these distinct organs are patterned from a shared oral epithelium, (*ii*) how diversity in organ density is achieved across closely related species, and (*iii*) which molecular pathways and genomic regions control patterning. Working from insights in the cichlid system, we explored the activity of novel candidate genes for tooth and taste bud patterning in the mouse model.

Significance

Teeth and taste buds are placode-derived organs studied in isolation because of their separate anatomical locations in mammals. Yet, the mouth and pharynx of many aquatic vertebrates, including bony fishes, are lined with teeth and taste buds, one next to the other. Using a combination of genome mapping, synexpression analysis, and small-molecule manipulation, we identify factors that couple tooth and taste bud density (Wingless signals) and those that differentiate the identity of each organ from a common epithelial lamina (BMP, Hedgehog). Integrating results from fishes and mouse suggests a model wherein the regulatory hierarchies that configure teeth and taste buds on mammalian jaws and tongues may be evolutionary remnants inherited from ancestors whose oral organs were copatterned from common epithelium.

Author contributions: R.F.B., P.T.S., and J.T.S. designed research; R.F.B., N.F.P., K.A.P., T.E.F., and T.Y.Y. performed research; and R.F.B., N.F.P., P.T.S., and J.T.S. wrote the paper.

The authors declare no conflict of interest.

This article is a PNAS Direct Submission.

Freely available online through the PNAS open access option.

Data deposition: The cDNA sequences reported in this paper have been deposited in the GenBank database (accession nos. KT851375–KT851399).

[1]To whom correspondence may be addressed. Email: rbloomquist@gru.edu or todd.streelman@biology.gatech.edu.

This article contains supporting information online at www.pnas.org/lookup/suppl/doi:10.1073/pnas.1514298112/-/DCSupplemental.

Results

Common Regions of the Cichlid Genome Contribute to a Positive Correlation Between Tooth and Taste Bud Density. The positive phenotypic correlation between tooth and taste bud density observed across Malawi cichlid species could be controlled by: (*i*) pleiotropy, wherein common genetic intervals control both tooth and taste bud density, and (*ii*) epigenetics (in the general sense), wherein the density of one of these structures constrains or determines the density of the other. To explore the genetic basis of tooth and taste bud densities, we assessed the correlation in F_2 fishes from an intercross between two rock-dwelling Lake Malawi cichlid species, *Cynotilapia afra* (CA), a planktivore with few teeth and taste buds and *Pseudotropheus elongatus* (PE), an algivore with many of both. Tooth and taste bud densities each ranged >fourfold and were positively correlated across F_2 (r^2 = 0.43) (*SI Appendix*, Fig. S1). To identify the genome intervals controlling tooth and taste bud density, we used a quantitative trait loci (QTL) mapping framework, using fully informative RAD-Tag single nucleotide polymorphisms (SNPs), as previously described for other phenotypes (15).

Briefly, we genotyped informative SNPs in the F_2 and constructed a genetic linkage map. We joined 370 loci in 22 linkage groups (Malawi cichlids have 22 haploid chromosomes) (16). The dataset exhibits nearly complete genotypes across 382 F_2 (0.4% missing data). The linkage map was translated to genome assemblies of tilapia, *Oreochromis niloticus* (an East African river cichlid) and *Metriaclima zebra* (MZ, another Lake Malawi rock-dwelling cichlid) (17). We used the assembled linkage map to determine QTL location and mode of effects for lower jaw tooth and taste bud densities in 263 F_2 animals with complete phenotypic data (*Materials and Methods*). We integrated single-QTL scans using standard and composite interval mapping with 2D scans to identify pairwise (epistatic) QTL interactions and built multiple QTL models (MQM) incorporating QTL interactions, as well as phenotypic sex as a potential covariate. Marker quality and size of the dataset give us suitable power to detect epistasis and sex-specific effects (15).

The final model for tooth density (logarithm of odds, LOD = 32.09) incorporated eight loci and three epistatic effects, accounting for 43% of the phenotypic variance in this trait (phenotypic variance explained, PVE = 43.11) (Fig. 1 and *SI Appendix*, Table S1). The largest effect was observed at position 5.8 cM on chromosome 11 (i.e., 11@5.8), explaining an estimated 15.52% of the phenotypic variance. This QTL was responsible for two of the three epistatic interactions for tooth density (plots of which are shown in *SI Appendix*, Fig. S2). Three other large- to moderate-effect loci were each associated with >8% of the variance in tooth density, cumulatively accounting for a large proportion of the PVE for this trait. Two of these QTL positions (17@34.8 and 20@51) were independently identified as genetic determiners of taste bud density (*SI Appendix*, Table S1). Three other loci and one epistatic interaction were included in the full MQM for taste bud density (LOD = 14.4, PVE = 22.35) (Fig. 1 and *SI Appendix*, Table S1). Unlike other oral jaw traits (15), here we did not detect a significant effect of phenotypic sex on either density measure. Allelic effects of QTL were observed with conflicting directions

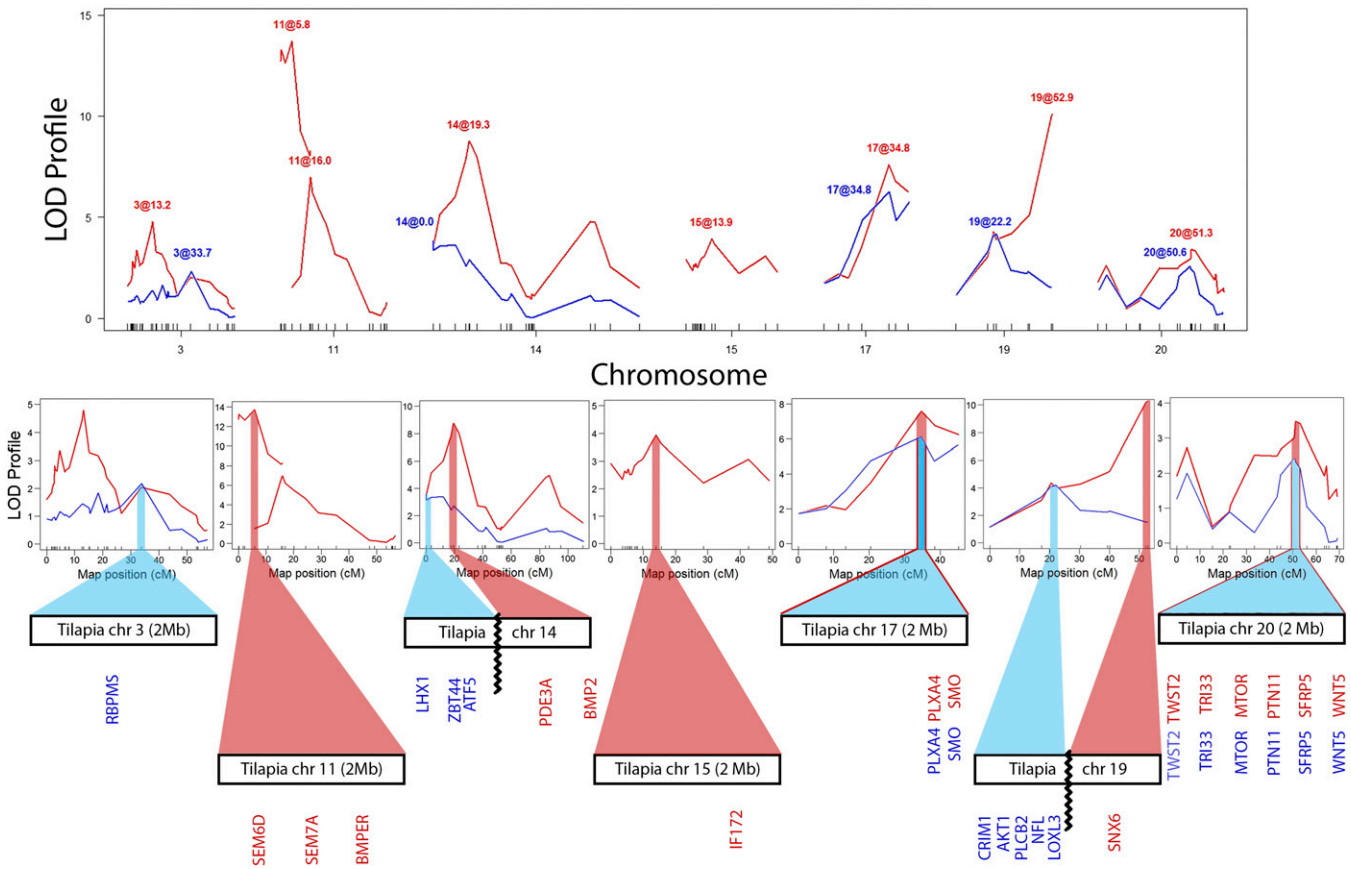

Fig. 1. QTL profile for significant tooth (red) and taste bud (blue) genetic effects, with chromosome position plotted against LOD score. Best-scoring SNP markers from MQM models were located in cichlid genomes and all annotated genes 1 Mb on either side were identified. (*Lower*) Candidate genes for tooth and taste bud density are indicated along expanded 2-Mb portion of the *x* axis approximately positioned from the center of the peak for tooth (red) and taste bud (blue). Note shared QTL for tooth and taste bud density on chromosomes 17 and 20.

for each density trait (e.g., CA/CA homozygotes for QTL 17@34.8 exhibited greater tooth density compared with PE/PE, but lower tooth density when indexed for locus 20@51); these plus and minus allelic effects may explain the transgressive trait distribution among F_2 (*SI Appendix*, Fig. S1). Notably, coincident QTL for tooth and taste bud densities (17@34.8 and 20@51) showed similar directions of effect across traits (i.e., CA/CA homozygotes indexed for 17@34.8 exhibited greater tooth and taste bud densities). Overall, these quantitative genetic data suggest that epistasis and pleiotropy (or genetic linkage) contribute to the observed positive correlation between tooth and taste bud densities in Malawi cichlids.

Using annotated cichlid genomes (17), we manually curated all predicted genes within one megabase in both directions (2 Mbp total) around the highest LOD-scoring SNPs from MQM models. We highlight positional candidate genes based on either (*i*) published interactions in placode-derived organ development or (*ii*) known roles in BMP, FGF, Hh, or Wnt pathways. Notable among these positional candidates is the gene *smo*, a well-known mediator of Hh signaling, in close proximity to 17@34.8, a QTL for both tooth and taste bud density; the gene *bmper*, a modulator of BMP activity, near the largest-effect QTL for tooth density (11@5.8); *bmp2*, well studied in tooth development, near a tooth density QTL (14@19.3); and genes *sfrp5* and *wnt5a*, effectors of Wnt/β-catenin signaling near the 20@51 tooth and taste density QTL.

Cichlid Tooth and Taste Bud Fields Are Specified from a Common Lamina. Because cichlid teeth and taste buds are colocalized on the jaw, we sought to understand the developmental ontogeny of each. In cichlids and other vertebrates, the earliest markers of the dental epithelium, or dental lamina, are *sonic hedgehog* (*shh*) and *pitx2* (14). Similarly, presumptive taste bud epithelium is known to express *sox2* and *shh* at the earliest stages (18, 19). We used in situ hybridization (ISH) at 5 d postfertilization (5 dpf) when the oral jaws first become apparent, to chart the spatial activity of these markers (Fig. 2). The earliest oral lamina expresses *pitx2* (a marker of dental epithelium), *shh* (a marker of dental and taste epithelium), and *sox2* (a marker of taste epithelium) with near-overlapping patterns in the rostral oro-pharynx (Fig. 2, black arrows), whereas *shh* and *sox2* occupy a more posterior domain (Fig. 2, white arrowhead). A day later (6 dpf), we observed the first $pitx2^+$, shh^+ dental placodes and the initiation of $calb2^+$ (a marker of mature taste buds with more distinct expression than *sox2*) taste buds forming lingual to them (*SI Appendix*, Figs. S3 and S4). Subsequently (7 dpf), a labial band of taste buds appears flanking the newly forming first row of teeth. Throughout, the epithelial dental field is circumscribed by the odd-skipped transcription factor *osr2* expressed in mesenchyme; *osr2* constrains tooth rows in mice (20). Successive rows of teeth will be added between lingual rows of taste buds as the animal matures (*SI Appendix*, Fig. S5). Therefore, each tooth row is flanked by labial and lingual bands of taste buds.

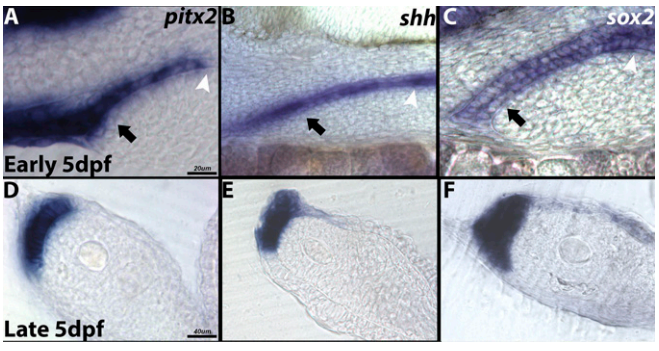

Fig. 2. Expression of *pitx2*, (*A* and *D*), *sox2* (*C* and *F*), and *shh* (*B* and *E*) at early stages of tooth and taste bud copatterning. Sagittal section at initial stages of jaw formation, early 5 dpf (20×; scale bar, 20 μm) and late 5 dpf (40×; scale bar, 40 μm). Black arrows show shared first arch lamina and white arrowhead shows reduced *pitx2* in posterior pharynx (*A*) compared with *shh* (*B*) and *sox2* (*C*). Rostral is to the left of page, ventral to the bottom; 18-μm-thick sections.

We focused on the stage of initial tooth and taste bud condensation (6 dpf) because this is the first point during which common epithelium becomes differentiated as either $pitx2^+$ tooth or $calb2^+$ taste buds. We therefore assayed the spatial expression by ISH of a number of placodal markers as well as genes in the BMP, FGF, Hh, and Wnt pathways, in both whole-mount and histological section (*SI Appendix*, Figs. S6 and S7, and Table S2). FGF signal plays known roles in the patterning of teeth and taste buds in the mouse (21, 22) and in the zebrafish pharynx (23, 24), but its function in the oral jaws of teleost fishes is less clear. Here, we observed *fgf10* in condensed dental mesenchyme, *fgf7* in the forming velum lingual to teeth/taste buds, and no activity of *fgf8* in the oral organ field (see also ref. 14). We detected *fgfr1* and *spry4* in the oral epithelium, consistent with the position of initial tooth and taste buds (*SI Appendix*, Fig. S7), suggesting that FGF signal is transduced in these placodes. *pax9*, known to be involved in the development of cichlid teeth (14) and mouse tongue papillae (18), was active throughout the mesenchyme subjacent to both tooth and taste bud fields. Wnt ligands *wnt7b* and *wnt10a* delineate and mark tooth placodes, respectively; *β-catenin* is expressed broadly across the tooth and taste epithelium; *shh* marks both the initial tooth placodes as well as the lingual taste bud field; the Hh receptor *ptc1* is broadly expressed; *sox2* is expressed in epithelium corresponding to lingual and labial taste bud fields, flanking the $pitx2^+$ tooth row. The BMP receptor, *bmpr2b*, is expressed diffusely in the epithelium of tooth placodes and the lingual taste field, and *bmp4* is strongly activated in both dental epithelium and mesenchyme. Notably, numerous BMP antagonists are expressed in the epithelium or mesenchyme marked for lingual and labial taste bud fields; this includes *ectodin* (*wise, sostdc*), *osr2*, and *fst*. Similarly, the Pitx2 repressor, *tbx1* (25), is strongly expressed lingual to the initial tooth row. Taken together, these data from gene expression suggest roles for the Hh, Wnt, and BMP pathways in copatterning of cichlid teeth and taste buds, and furthermore that BMP signaling promotes the differentiation of teeth from a common epithelial field, whereas multiple BMP and *pitx2* antagonists are protective of $sox2^+$, $calb2^+$ taste domains.

Positional Candidate Genes Are Expressed in Teeth and Taste Buds of Fishes and Mice. We examined the expression of positional candidate genes from QTL analysis (above) during the placode condensation stage (*SI Appendix*, Figs. S6 and S7, *Inset*). *smo*, a coreceptor in the Hh pathway, near a coincident QTL for tooth and taste bud density, was expressed generally throughout the jaw epithelium, except in the primary dental placodes. As observed in the mouse (26), this transcript was not detectable at later stages. *bmp2* and *wnt5a*, near tooth and taste bud density QTL, are expressed in dental epithelium and mesenchyme, or in the mesenchyme flanking dental and taste placodes, respectively. *sfrp5* and *bmper* are interesting positional candidate genes because they have not been heavily studied in oral placode development. Both are expressed in mesenchyme in complementary antitooth patterns. *sfrp5* has been described as a Wnt inhibitor in several systems (27, 28), an integrator of Wnt-BMP signaling in the zebrafish gut (29), and a regulator of mouse incisor renewal (30). *bmper* has been reported as both a positive and negative mediator of BMP signaling in other organs of the mouse, frog, and fly (31–33), and as an antagonist of BMP in mouse incisor ameloblasts (34). We assayed expression of these candidates in species with divergent densities of teeth/taste buds: *C. afra*, a

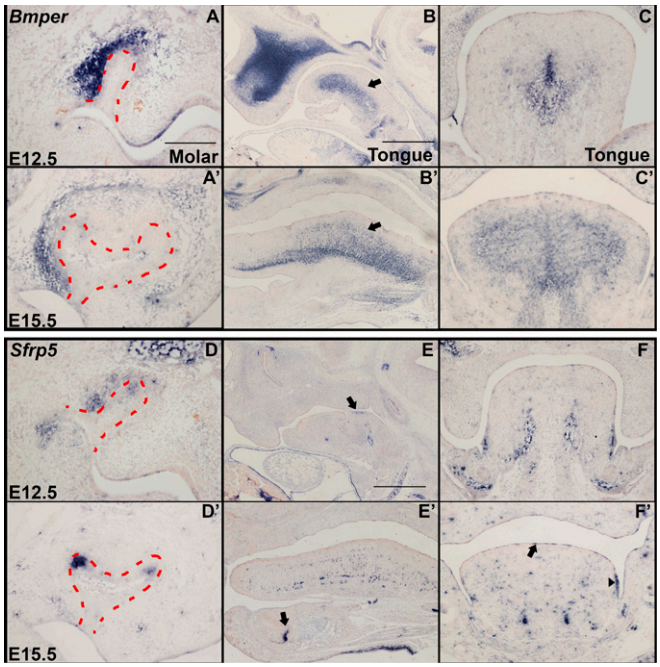

Fig. 3. Expression of candidates *Bmper* and *Sfrp5* in mouse teeth and tongues. *Bmper* and *Sfrp5* expression, as shown in frontal section of bud stage molar teeth at E12.5 (*A* and *D*) and cap stage teeth at E15.5 (*A′* and D′) (20×). (Scale bar, 200 μm.) Gene expression in tongue as observed in sagittal (*B*, *B′*, *E*, and *E′*) and frontal (*C*, *C′*, *F*, and *F′*) sections at E12.5 and E15.5, respectively (10×) (Scale bar, 400 μm.)

species with few teeth and taste buds and *Labeotropheus fuelleborni*, a species with many of both (*SI Appendix*, Fig. S8). *bmper* is expressed diffusely in bands flanking the tooth field; expression is stronger in *C. afra*. Notably, *sfrp5* is expressed from the midline in a gradient that encompasses much of the tooth and taste bud fields of both species; expression is strongest and broadest in *C. afra*. These expression differences between species are consistent with antagonistic roles for each gene in BMP (*bmper*) and Wnt (*sfrp5*) signaling, at this stage.

Because these genes have not been well studied in mammal tooth and taste bud development, we assessed gene expression by ISH in teeth on mouse jaws and taste buds on mouse tongues (Fig. 3). *Bmper* expression, observed at the molar bud stage [embryonic day (E) 12.5] was restricted to buccal mesenchyme, a pattern similar to that of *Bmp4* (Fig. 3*A*) (35). By E15.5, expression can be seen surrounding the cap stage tooth bud in mesenchyme, in areas corresponding to the sites of osteogenesis (Fig. 3*A′*). The highest expression level was still observed in buccal mesenchyme, adjacent to the dental epithelium. *Bmper* expression in the developing tongue was restricted to the deeper mesenchyme in the areas where musculature develops (Fig. 3 *B*, *B′*, *C*, and *C′*). *Sfrp5* was also observed predominantly in buccal molar tooth mesenchyme at the bud stage, with some expression in the epithelium at the tip of the bud (Fig. 3*D*). At E15.5, mesenchymal expression of *Sfrp5* is largely undetectable but highly restricted expression was located in the epithelium of the cervical loop with a greater level in the buccal aspect (Fig. 3*D′*). In the tongue, *Sfrp5* expression was weak and diffuse except for a small area corresponding to the single circumvallate papilla that also expresses *Wnt10b* (Fig. 3*E*) (9). By E15.5, punctate expression in the deep tongue mesenchyme was observed (Fig. 3*E′*) with localized expression on the dorsal and lateral epithelial surfaces corresponding to (Fig. 3*F′*). In addition *Sfrp5* was expressed in the incisor cervical loop (Fig. 3*E′*).

Manipulation of Signaling Reveals Epithelial Plasticity via a Complex Logic of Placode Specification. QTL and gene-expression data implicate the Wnt, BMP, and Hh pathways in the regulation of tooth and taste bud densities, as well as the patterning of these organs from a common oral epithelium. To test the precise role of these pathways, we used small-molecule antagonists to modulate signaling during the placode condensation stage. We applied LDN-193189 (LDN), an inhibitor of the BMP pathway; endo IWR-1 (IWR), an antagonist of the Wnt pathway; and cyclopamine (CYC), an antagonist of the Hh pathway, in fishwater at 6 dpf for 24 h. Split broods received small molecules or vehicle control. Following chemical or sham treatment, a subset of embryos was washed, returned to fishwater, and allowed to develop until euthanized (36) at 14 dpf, for quantification of tooth and taste bud densities. A second subset of embryos was euthanized immediately after

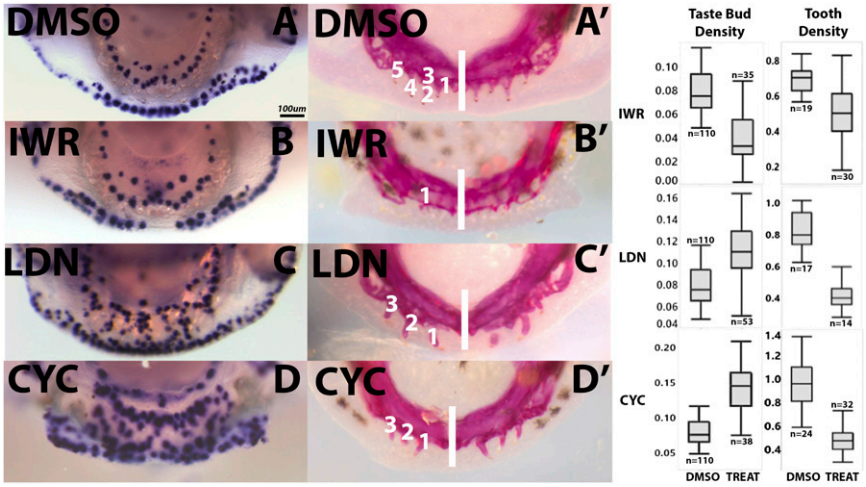

Fig. 4. Effects of chemical treatment on tooth and taste bud density. *calb2* ISH was used to score taste bud density (*A*–*D*) and cleared and stained jaws were used to score tooth density (*A′*–*D′*). The midline of cleared and stained fish is marked by a white line; teeth in each half of the dentary are marked by white numerals. Dorsal views of dentaries, labial to bottom of page. (Scale bars, 100 μm.) Box plots summarize statistical analysis of chemical treatments vs. control (DMSO), for taste buds (no. of taste buds per 10 μm^2) and teeth (no. of teeth per 100 μm^2). All treatments are significantly different from control, with $P < 0.0001$; n = numbers of animals used.

treatment, followed by ISH to examine the effects of pathway manipulation on gene expression.

Treatment with IWR significantly reduced the density of teeth and taste buds, compared with control siblings (Fig. 4) ($P < 0.0001$). Abrogated or reduced expression levels of *sox2*, *pitx2*, BMP-, and Hh-pathway members likely mediate this effect on both oral organs, observed after 24 h of treatment (*SI Appendix*, Fig. S9). In the set of genes we assayed, the only one whose expression increased or expanded after IWR treatment was the putative Wnt antagonist, *sfrp5*. Notably, we raised a small number of IWR-treated animals to 1 mo and noted a lasting reduction in the density of teeth and taste buds (*SI Appendix*, Fig. S10). LDN treatment (knockdown of BMP signaling) resulted in a striking increase in taste bud density at the expense of tooth density (Fig. 4) ($P < 0.0001$). In LDN-treated animals, taste papillae invaded the tooth field and occupied interdental spaces, suggesting the breakdown of developmental boundaries. It is possible that *calb2*$^+$ cells migrated to occupy the normally obligate tooth field, or that the oral epithelium holds inherent plasticity at this juncture. Observations of gene expression 24 h after treatment support the latter notion (Fig. 5). LDN treatment resulted in reduced expression of dental placode transcription factors *pitx2* and *lef1*, and dramatic expansion of *sox2* and *shh* into the tooth field. *calb2*$^+$ taste papilla development was accelerated and the putative BMP antagonists *osr2* and *bmper* showed up-regulation and expanded spatial domains, as observed for *Osr2* in mouse conditional *Bmp4* knockouts (37). Similar to knockdown of BMP signaling, Hh antagonism via temporary CYC treatment reduced the density of teeth and increased the density of taste buds, compared with controls (Fig. 4) ($P < 0.0001$). This appears to be mediated by an increase in both lingual and labial taste bud fields coincident with a smaller dental domain. After just 24 h, CYC almost completely abolished expression of the *ptch1* receptor (Fig. 5). As in LDN treatment, CYC exposure yielded an expansion of taste bud markers *calb2* and *sox2* at the expense of the *pitx2*$^+$ tooth field. Expression of the transcription factor *pax9* was reduced; we noted negligible effects on *bmp2* expression.

Finally, to assay if ectopic taste buds in taste and dental fields after LDN and CYC treatment held potential for functional activity, we used double whole-mount immunohistochemistry against; (*i*) acetylated-Tubulin (Fig. 6, red), a marker of innervation (38), and (*ii*) calretinin/Calb2 (Fig. 6, green) and visualized fluorescence using nonlinear optics in conjunction with multiphoton microscopy. Taste buds that invade the tooth field after LDN treatment were well innervated, but following CYC treatment their counterparts were not (Fig. 6, arrows). Recent study in adult mice shows that mis-expression of Shh is sufficient to induce ectopic taste placode development in lingual regions of the tongue, surprisingly independent of innervation (39). That data, in conjunction with ours, highlight differing roles of Hh and innervation in embryonic development versus adult maintenance of taste placodes (40).

To sum up, our treatment data demonstrate that when teeth and taste buds are patterned from common epithelium, Wnt signaling exerts a positive influence on the densities of both organs, whereas BMP and Hh signaling both promote, or reinforce, the development of teeth. Assessment of gene expression after treatment suggests that the Wnt pathway acts upstream of BMP and Hh as teeth and taste buds initiate development. Notably, the epithelial plasticity (or bipotency) revealed from both LDN and CYC treatments may be a common feature of organ systems like teeth and taste buds that function together, as observed for liver and pancreas (41), and hearts and lungs (42).

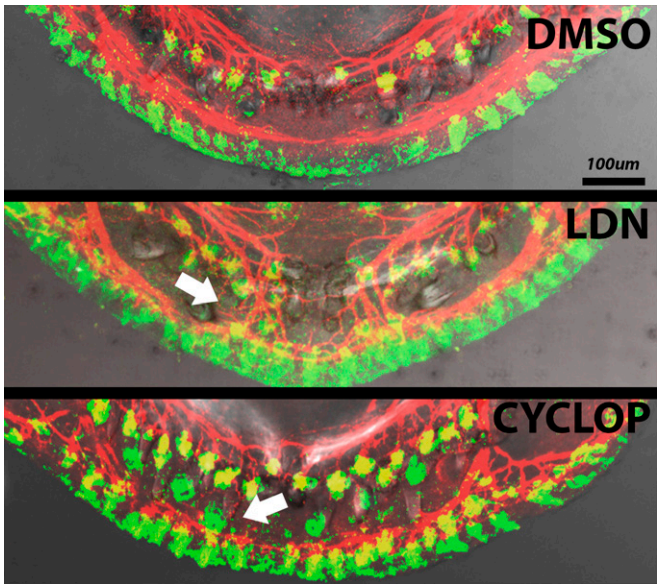

Fig. 6. Dorsal views of dentary after whole-mount IHC of taste bud marker Calb2 (green) and nerve marker acetylated Tubulin (red) following LDN or CYC treatment. Three-dimensional rendering of 150-μm optical sections overlaid to bright-field image at 10×. White arrows indicate ectopic taste bud. Labial to bottom of page. (Scale bar, 100 μm.)

Discussion

Deep Ancestry of the Wnt-BMP-Hh Regulatory Hierarchy in Oral Placode Development. In many vertebrates, teeth and taste buds are colocalized in the oro-pharyngeal cavity and function together as potential food items are assessed, acquired, and then (in some cases) masticated. In Malawi cichlids, the number and density of teeth and taste buds varies widely (14) and the positive phenotypic correlation between tooth and taste bud densities makes adaptive sense. Planktivores typically assess food/prey using acute vision and swallow it whole; they tend to have reduced tooth and taste bud densities. In contrast, algivores use taste and smell to make food choices and then use flexible or shearing teeth to comb or nip from the substrate: they generally possess many teeth and many taste buds.

We showed here that the phenotypic correlation between tooth and taste bud densities is, at least partly, explained by genetic variants in common regions of the cichlid genome. We identified

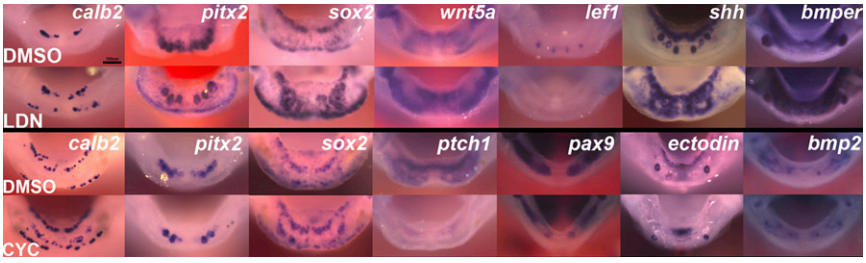

Fig. 5. ISH of genes in cichlid dentary following 24-h treatment with LDN or CYC initiated at 6 dpf and immediate euthanasia. Dorsal views, labial to bottom of page. (Scale bar, 100 μm.)

positional candidate genes in the BMP, Hh, and Wnt pathways whose gene expression in fishes and mouse suggest largely conserved roles in the patterning of teeth and taste buds, regardless of whether these organs are colocalized from common epithelium (fish), or located in spatially restricted parts of the mouth (mouse). Using QTL and gene-expression data as a lead, we manipulated BMP, Hh, and Wnt pathways and demonstrated that Wnt signaling couples the density of teeth and taste buds, whereas BMP and Hh signaling promote the development of teeth at the expense of taste buds, at these early stages. QTL analysis revealed genetic interaction, and positional candidate genes with differential expression in species possessing low vs. high tooth and taste bud densities. Future efforts will focus on the enhancer regions that drive developmental differences in expression across oral epithelium and mesenchyme, as well as the precise role of epistasis in regulating oral organ density.

Taken together, our observations are notable for two reasons. First, manipulation of Wnt signaling in cichlids produces a positive correlation between tooth and taste bud densities, similar to the correlation we observe across natural species and in the F_2 of our intercross. Modulation of Wnt signaling early in the development of cichlid teeth and taste buds is sufficient to phenocopy natural differences among cichlid species (*SI Appendix*, Fig. S10). Second, our small-molecule treatment experiments, followed by assays of gene expression, suggest that Wnt acts upstream of BMP and Hh in the copatterning of tooth and taste bud fields from common epithelium. Therefore, the function of these pathways, their mode of effects, as well as their relative position in a regulatory hierarchy, is strikingly consistent between fishes and mammals, given the noteworthy spatial difference in organ distribution (Fig. 7). In cichlids, Wnt signal promotes the initiation of both organs, as well as BMP and Hh from a bipotent epithelium. As tooth and taste placodes mature, distinct fields develop wherein taste buds are patterned initially in a proximal or lingual zone to the tooth field and are recruited by Wnt signals, but repressed by BMP and Hh elsewhere. In contrast all three pathways synergistically support the maturation of tooth placodes distally. It is well established in other model organisms that teeth and taste buds are derived in part from ectomesenchyme of neural crest origin (43, 44). In cichlids, neural crest-derived ectomesenchyme is likely induced to the placodes under a BMP^+ tooth environment expressing *bmp2/4* and a BMP^- taste environment, restricted by repressors like *osr2* and possibly *bmper*. It is likely that factors expressed by maturing tooth and taste buds are in turn restrictive of one another and help delineate the respective fields (Fig. 7).

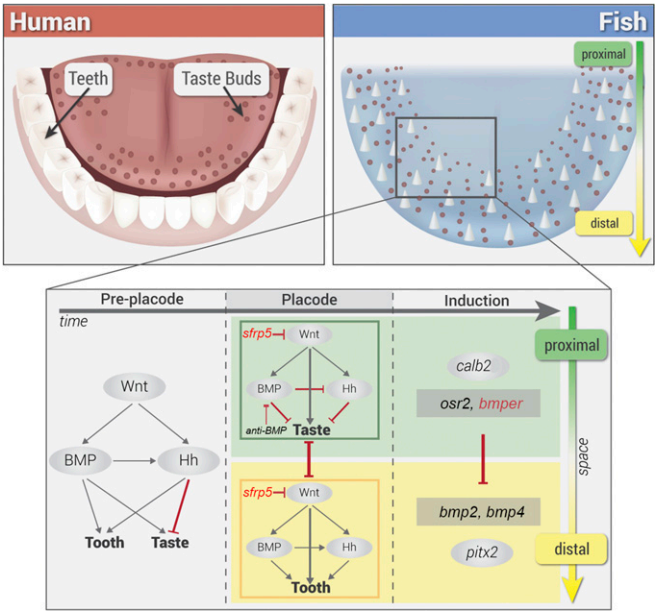

Fig. 7. A model of evolutionary conserved patterning networks for oral organs. Humans possess taste buds on the tongue and teeth on the dental arch, whereas these organs are copatterned in cichlids and other fishes. Inferred roles of Wnt-BMP-Hh interactions and effects on tooth and taste bud patterning in cichlids represented before placode condensation, during placode formation, and during induction of mesenchyme to both organs, from proximal to distal of horizontal plane. Genomic candidates are highlighted in red text. Preplacode stage represents the model of placode recruitment from a bipotent epithelium. These interactions are consistent with reports in the mouse for taste bud (9, 11, 70) and tooth (8, 21, 38, 47, 49) patterning networks, when studied independently. Based on cichlid expression and treatment data, Wnts drive the formation of taste placodes proximally and tooth placodes distally, whereas BMPs and Hhs are inhibitory of taste bud differentiation and permissive for tooth germs. Anti-BMPs, such as *osr2*, may reduce BMP activity in the taste field to promote taste bud formation and *sfrp5*, expressed in both fields, may repress Wnt signaling. At the point of mesenchyme induction, *pitx2* is expressed in tooth placodes and the underlying mesenchyme expresses *bmp2/4*. Simlarly, taste buds express *calb2* and anti-BMPs *osr2* and *bmper* are expressed in the lingual mesenchyme.

In the mouse, the Wnt/β-catenin signal is one of the earliest markers of dental placodes on the jaw margin and taste placodes on the tongue, acting upstream of BMP and Hh in both organs (10, 11). Up-regulation of Wnt signaling in the mouse dentition, via constitutive activation of β-catenin or genetic ablation of Apc, leads to extra teeth (45, 46). Similarly, culture of mouse tongues with LiCl, an agonist of Wnt/β-catenin, and the activating β-catenin mutation, both increase taste papillae number and size (9, 11). Hh signaling is necessary for proper development of teeth in fishes and mammals (14, 47) and ectopic activity in the mouse diastema leads to extra teeth (48). Culture of mouse tongues with 5E1, an antibody against Shh leads to more papillae; culture with purified Shh reduces papillae number (9). Numerous reports using gene targeting have shown that ablating function of BMP antagonists [Ectodin (Sostdc1, Wise) (49), Noggin (50), Osr2 (20)] increases tooth number. Similarly, ectopic expression of the BMP antagonist Follistatin, using the K14 promoter, reduces tooth number (51). BMP data for mammalian taste papillae are complicated and stage-specific. A variety of BMPs are expressed in mammalian tongue papillae with considerable variation across stages (52). Zhou et al. (53) report that culture of rat tongues with purified BMPs or the antagonist Noggin at E13 results in increased numbers of taste papillae, but that treatment at E14 with BMPs decreases papillae, whereas Noggin treatment increases them. Interestingly, genetic ablation of Follistatin increases BMP signal in the mouse tongue and gives rise to ectopic posterior papillae that express *Sox2* and *Foxa2*, but which appear to invaginate rather than evaginate like typical taste buds (54). Overall, teeth and taste buds share gene synexpression and a deep molecular homology (12). Our work here implies that the Wnt-BMP-Hh regulatory hierarchy patterning these organs is conserved, despite release from the constraint of spatial colocalization in mammals (and other vertebrates). The conservation of regulatory interactions is a well-known tenet of development for homologous structures [e.g., the heart (55)], and core regulatory circuits are sometimes used in different organs, such as the case of Pax-Dach-Eya-Six in eye and muscle development (56). We highlight a special case of conservation in evolutionary development, wherein the function and interaction of signaling in independent regulatory networks (to make teeth on the mammalian jaw margin and taste buds on the tongue) may be evolutionary remnants of a single gene circuit that evolved long ago to copattern these organs from common oral epithelium.

Materials and Methods

Cichlid Husbandry. Species of Lake Malawi cichlids used in this analysis include: *Tramitichromis intermedius* (TI), *C. afra*, *L. fueleborni* (LF), *M. zebra*, *Petrotilapia chitimba* (PC), and *P. elongatus*. These species were chosen to represent diversity in tooth and taste bud densities. Adult cichlids were maintained in recirculating aquarium systems at 28 °C (GIT). Fertilized embryos were removed from the mouths of brooding females and staged in days post-fertilization according to Nile Tilapia developmental series (57). Embryos were raised to desired stages for chemical treatment or euthanized with MS-222 for fixation in 4% paraformaldehyde followed by dehydration into MeOH.

Mouse Husbandry. Outbred CD1 mice were obtained from Charles River. Noon of the day when a vaginal plug was detected was designated as E0.5. Time-mated embryos were collected at E12.5, E13.5, and E15.5. All mouse procedures were approved by the United Kingdom Home Office.

Tooth and Taste Bud Phenotyping in Cichlid Species and F_2. Following euthanasia (Institutional Animal Care and Use Committee standard protocol A11035) measurements of standard length (nearest millimeter) were taken on each individual and the dentary was dissected in 70% (vol/vol) EtOH. Jaws were rehydrated in reverse osmosis purified water (60 s) and immersed in Toluidine blue for 60 s to visualize taste buds (58). The dentary was photographed at 7–16× on a Leica MZ16 dissecting microscope with a scale bar merged to each photo. Taste buds (found in the shared epithelial field, see below) were counted in ImageJ (59) using the cell counter plugin. Jaws were then cleared with KOH and glycerin using standard protocols (60) to allow accurate counts of all teeth (erupted and replacement teeth) as well as measurement of the tooth/taste field. Each dentary was then photographed again as described above, without staining. Tooth counts were made using ImageJ (59). The tooth/taste bud field was quantified by calibrating the scale bar in ImageJ and creating a polygon extending around the entire field; this delineation thus included the area in which teeth and taste buds were quantified. Total tooth and taste bud counts were divided by total shared tooth/taste bud field area to account for any differences in jaw size because of allometry.

QTL Mapping of Cichlid Tooth and Taste Bud Densities. We used RAD-tag SNPs to map tooth and taste bud densities in F_2 animals, as described previously for other phenotypes (15, 61), with one important addition: from genome-anchored linkage maps of *O. niloticus* and *M. zebra* (17), we handpicked an additional set of SNPs predicted to fill gaps in linkage group coverage. This second group of SNPs was genotyped in the same F_2 population using the Fluidigm Dynamic Array (15). This resulted in a fully informative set of SNP markers covering the cichlid genome, with nearly complete genotypic data across F_2 (0.4% missing data). A genetic linkage map was constructed with SNP marker genotype data using JoinMap 3.0 software, as described previously (15). The map was created using Kosambi's mapping function, a LOD threshold of 1.0, a recombination threshold of 0.4, a jump threshold of 6.0, and a ripple function with no fixed order of loci. A LOD threshold of 4.0 was used to join 370 loci in 22 linkage groups with a total map size of 1,381 cM and average marker distance 4.38 ± 1.85 cM, with an average of 16.8 markers per linkage group. To facilitate comparison with other genetic maps in Malawi (62–65) as well as tilapiine cichlids (66), our linkage group names represent consensus cichlid chromosomes.

The linkage map was used to determine genomic locations for tooth and taste bud densities in the F_2 population using the R/qtl package (67). We used an iterative approach by scanning for single QTL with standard and composite interval mapping, followed by 2D scans to identify QTL × QTL interactions (i.e., epistasis) and detect additional QTL. Using results of the previous steps we built MQM incorporating QTL interactions and potential covariates (i.e., sex). In the MQM process, we used a forward-backward selection algorithm to add and remove QTL based on overall model effects and the effects of single QTL as they were removed from the model (termed drop-one). This approach allows user input (e.g., from single and 2D scans) combined with the automated cofactor search implemented in R/qtl. During each iteration, QTL positions and effects are refined, in the context of the overall MQM. Genotype–phenotype associations are scored using the LOD, which represents the $\log_{10}$ likelihood ratio comparing the hypothesis of a QTL at a marker location to the null hypothesis of no QTL [$\text{LOD} = (n/2)\log_{10}(\text{RSS}_0/\text{RSS}_1)$], where RSS is residual sum of squares (67). The variance in a phenotype is assigned to each significant QTL (or covariate) and reported as PVE in the analysis output. The total variance accounted for by QTL is a proxy for the heritability of a trait and is calculated as $1 - 10^{-(2/n)\text{LOD}}$ (67). Significance thresholds for LOD scores were estimated using 1,000 permutations of phenotypes relative to genotypes to build a distribution of maximum genome-wide LOD scores. From this distribution, the 95th percentile LOD score was calculated to serve as a threshold for significant QTL associations in the drop-one analysis (67).

To identify positional candidate genes, we manually curated all predicted genes within 1 Mb up- and downstream from the highest LOD-scoring SNPs from MQM models, using annotated cichlid genomes (17). Candidates were selected based on published interactions in placode-derived organ development or a known relationship to BMP, Hh, Wnt, or FGF signaling pathways.

Cichlid ISH. Digoxigenin-labeled antisense riboprobes were prepared using partial cichlid genome assemblies (68), as well as recently assembled tilapia and *M. zebra* genomes (17). DNA sequence diversity across the Lake Malawi assemblage is 0.28%; less than reported values for laboratory strains of zebrafish. cDNA sequences for probe design have been deposited in GenBank (accession nos. KT851375–KT851399). ISH was performed according to previously published protocols (14, 69). Embryos were rehydrated from MeOH and ISH was carried out in whole-mount. Digoxigenin-labeled antisense riboprobes were generated using the Riboprobe System Sp6/T7 kit (Promega). AP-conjugated anti-dig antibodies were visualized at the end of color reaction (NBT/BCIP; Roche) using Leica MZ16 dissecting microscope. Embryos were embedded in chick albumin cross-fixed with 2.5% (vol/vol) gluteraldehyde and postfixed with 4% (wt/vol) PFA. A Leica Microsystems VT1000 vibratome was used to cut sections at 15–25 μm. Histological sections were then mounted with glycerine and imaged at 10–63× using a Leica DM2500 compound microscope.

Mouse Histology and ISH. Embryos were dissected in ice-cold PBS, fixed in 4% PFA overnight at 4 °C, before embedding in paraffin wax. Serial sections of the embryo were obtained at 10 mm and dried overnight at 42 °C. ISH was carried out using standard methods (70). Digoxigenin-labeled antisense probes for *Sfrp5* (IMAGE ID 1395864) and *Bmper* (IMAGE ID 3483063) were used. After completion of the color reaction, sections were counterstained with nuclear fast red, dehydrated, and mounted with DPX.

Treatment of Cichlid Embryos with Small Molecules. Stock solutions were prepared for each chemical treatment experiment using DMSO (MP Biomedicals). Stock solutions were as follows: 10 μm LDN-193189 (Enzo) in DMSO, 50 mM endo IWR-1 (Enzo) in DMSO, and 16 mM CYC (LC Laboratories) in DMSO. Cichlids were raised to 6 dpf and embryos from single broods were split into small molecule and solvent control groups. All chemical and control experiments were performed in Erlenmeyer flasks at 28 °C in an oscillating platform culture incubator (Barnstead Lab-Line Max 4000). Treatments were performed at 1.5 μM LDN, 3.75 μM IWR, and 2.5 μM CYC. After 24-h treatment in the small-molecule dilution, fry were euthanized immediately. ISH was carried out on experimental animals to understand effects of treatment on gene expression.

Alternatively, embryos were washed extensively with fresh fish water and raised to 14 dpf for euthanasia to understand effects of treatment on organ densities. Embryos were fixed and were either cleared and stained to assay effects of treatment on tooth density or ISH for the taste marker *calb2* was performed to assay effects of treatment on density of taste papillae. Tooth and taste densities were measured in different animals because the clearing/staining process and ISH damaged the tissues in combination. Posttreatment and staining, dentaries were photographed using a Leica MZ16 dissecting scope. Teeth (C&S) or taste buds (*calb2* ISH) were counted manually using ImageJ software, and jaw size was calculated using the measure function which converted pixel area of scale bar to millimeters. Total tooth and taste bud counts were divided by jaw area to account for possible size differences between specimens. All measurements for taste bud controls were pooled because experiments were conducted in the same species (*P. chitimba*), whereas those for tooth density were analyzed separately because experiments were conducted in different species (IWR, *P. chitimba*; LDN/CYC, *M. zebra*). Data were organized into box plots for each treatment set using JMP 11.0 software. Mann–Whitney *U* nonparametric tests were performed to test the null hypothesis of equal organ densities between treatment and control.

Cichlid Whole-Mount Immunohistochemistry and Nonlinear Optics Microscopy. For IHC, embryos were euthanized and fixed in 10% (vol/vol) NBF for 24 h at room temperature. Antigen retrieval was performed by washing 3 × 10 min. PBS, placing in 2β-mercaptonol for 1 h, washing in PBS, and incubating at 70 °C 150 mM Tris·HCl for 1 h. Embryos were incubated in blocking solution [3% (vol/vol) goat serum, 1% bovine serum, 0.1% Triton-X 100] for 3 h at room temperature, followed by 48-h incubation in a 1:1,000 dilution of rabbit anticalretinin (Millipore) and mouse IgG antiacetylated tubulin (Sigma) at 4 °C in blocking solution. Embryos were then washed 6× 1 h at room

temperature in PBS and incubated 24 h at 4 °C in 1:400 Alexa-Fluor 488 goat anti-rabbit IgG (Molecular Probes) and Alexa-Fluor 568 goat anti-mouse IgG (Molecular Probes). Unbound secondary antibody was removed by washing 48 h in PBS and specimen were stored in a 50:50 glycerin:Vectashield mixture for imaging. Deep-tissue whole-mount fluorescence was imaged by mounting embryos on glass depression slides and scanning with nonlinear optics using a Zeiss 710 system coupled with multiphoton microscopy. Conjugated antibodies were excited with a Coherent Chameleon Ti:Sapphire laser at 780 nm and scanned at their respective wavelengths.

ACKNOWLEDGMENTS. We thank members of the J.T.S. and P.T.S. laboratories for comments on previous drafts of this manuscript; Melissa Kinney for help in drafting Fig. 7; and Zach Marion for help with *SI Appendix*, Fig. S1. This study was funded in part by National Institute for Dental and Craniofacial Research Grants 2R01DE019637 (to J.T.S.) and 5F30DE023013 (to R.F.B.).

1. Hughes MW, Chuong CM (2003) A mouthful of epithelial–mesenchymal interactions. *J Invest Dermatol* 121(6):vii–viii.
2. Tucker A, Sharpe P (2004) The cutting-edge of mammalian development; how the embryo makes teeth. *Nat Rev Genet* 5(7):499–508.
3. Kondo S, Miura T (2010) Reaction-diffusion model as a framework for understanding biological pattern formation. *Science* 329(5999):1616–1620.
4. Sick S, Reinker S, Timmer J, Schlake T (2006) WNT and DKK determine hair follicle spacing through a reaction-diffusion mechanism. *Science* 314(5804):1447–1450.
5. Mou C, et al. (2011) Cryptic patterning of avian skin confers a developmental facility for loss of neck feathering. *PLoS Biol* 9(3):e1001028.
6. Cho S-W, et al. (2011) Interactions between Shh, Sostdc1 and Wnt signaling and a new feedback loop for spatial patterning of the teeth. *Development* 138(9):1807–1816.
7. Mikkola ML, Millar SE (2006) The mammary bud as a skin appendage: Unique and shared aspects of development. *J Mammary Gland Biol Neoplasia* 11(3-4):187–203.
8. Ahn Y, Sanderson BW, Klein OD, Krumlauf R (2010) Inhibition of Wnt signaling by Wise (Sostdc1) and negative feedback from Shh controls tooth number and patterning. *Development* 137(19):3221–3231.
9. Iwatsuki K, et al. (2007) Wnt signaling interacts with Shh to regulate taste papilla development. *Proc Natl Acad Sci USA* 104(7):2253–2258.
10. Liu F, et al. (2008) Wnt/β-catenin signaling directs multiple stages of tooth morphogenesis. *Dev Biol* 313(1):210–224.
11. Liu F, et al. (2007) Wnt-beta-catenin signaling initiates taste papilla development. *Nat Genet* 39(1):106–112.
12. Fraser GJ, Cerny R, Soukup V, Bronner-Fraser M, Streelman JT (2010) The odontode explosion: The origin of tooth-like structures in vertebrates. *BioEssays* 32(9):808–817.
13. Yamamoto Y, Byerly MS, Jackman WR, Jeffery WR (2009) Pleiotropic functions of embryonic sonic hedgehog expression link jaw and taste bud amplification with eye loss during cavefish evolution. *Dev Biol* 330(1):200–211.
14. Fraser GJ, Bloomquist RF, Streelman JT (2008) A periodic pattern generator for dental diversity. *BMC Biol* 6:32.
15. Parnell NF, Hulsey CD, Streelman JT (2012) The genetic basis of a complex functional system. *Evolution* 66(11):3352–3366.
16. Poletto AB, et al. (2012) Chromosome differentiation patterns during cichlid fish evolution. *BMC Genet* 13(1):2.
17. Brawand D, et al. (2014) The genomic substrate for adaptive radiation in African cichlid fish. *Nature* 513(7518):375–381.
18. Okubo T, Pevny LH, Hogan BL (2006) Sox2 is required for development of taste bud sensory cells. *Genes Dev* 20(19):2654–2659.
19. Hall JM, Hooper JE, Finger TE (1999) Expression of sonic hedgehog, patched, and Gli1 in developing taste papillae of the mouse. *J Comp Neurol* 406(2):143–155.
20. Zhang Z, Lan Y, Chai Y, Jiang R (2009) Antagonistic actions of Msx1 and Osr2 pattern mammalian teeth into a single row. *Science* 323(5918):1232–1234.
21. Neubüser A, Peters H, Balling R, Martin GR (1997) Antagonistic interactions between FGF and BMP signaling pathways: A mechanism for positioning the sites of tooth formation. *Cell* 90(2):247–255.
22. Petersen CI, et al. (2011) FGF signaling regulates the number of posterior taste papillae by controlling progenitor field size. *PLoS Genet* 7(6):e1002098.
23. Jackman WR, Draper BW, Stock DW (2004) Fgf signaling is required for zebrafish tooth development. *Dev Biol* 274(1):139–157.
24. Kapsimali M, et al. (2011) Fgf signaling controls pharyngeal taste bud formation through miR-200 and Delta-Notch activity. *Development* 138(16):3473–3484.
25. Cao H, et al. (2010) Tbx1 regulates progenitor cell proliferation in the dental epithelium by modulating Pitx2 activation of p21. *Dev Biol* 347(2):289–300.
26. Du J, et al. (2012) Expression of smoothened in mouse embryonic maxillofacial development. *Biotech Histochem* 87(3):187–194.
27. Li Y, et al. (2008) Sfrp5 coordinates foregut specification and morphogenesis by antagonizing both canonical and noncanonical Wnt11 signaling. *Genes Dev* 22(21): 3050–3063.
28. Suzuki H, et al. (2004) Epigenetic inactivation of SFRP genes allows constitutive WNT signaling in colorectal cancer. *Nat Genet* 36(4):417–422.
29. Stuckenholz C, et al. (2013) Sfrp5 modulates both Wnt and BMP signaling and regulates gastrointestinal organogenesis [corrected] in the zebrafish, *Danio rerio*. *PLoS One* 8(4):e62470.
30. Juuri E, et al. (2012) Sox2+ stem cells contribute to all epithelial lineages of the tooth via Sfrp5+ progenitors. *Dev Cell* 23(2):317–328.
31. Ikeya M, et al. (2006) Essential pro-Bmp roles of crossveinless 2 in mouse organogenesis. *Development* 133(22):4463–4473.
32. Moser M, et al. (2003) BMPER, a novel endothelial cell precursor-derived protein, antagonizes bone morphogenetic protein signaling and endothelial cell differentiation. *Mol Cell Biol* 23(16):5664–5679.
33. Kelley R, et al. (2009) A concentration-dependent endocytic trap and sink mechanism converts Bmper from an activator to an inhibitor of Bmp signaling. *J Cell Biol* 184(4): 597–609.
34. Cao H, et al. (2013) The Pitx2:miR-200c/141:noggin pathway regulates Bmp signaling and ameloblast differentiation. *Development* 140(16):3348–3359.
35. Vainio S, Karavanova I, Jowett A, Thesleff I (1993) Identification of BMP-4 as a signal mediating secondary induction between epithelial and mesenchymal tissues during early tooth development. *Cell* 75(1):45–58.
36. Clark JD, et al. (1996) *Guide for the Care and Use of Laboratory Animals* (Institute of Laboratory Animal Resources, National Research Council 125, Washington, DC).
37. Jia S, et al. (2013) Roles of Bmp4 during tooth morphogenesis and sequential tooth formation. *Development* 140(2):423–432.
38. LeClair EE, Topczewski J (2010) Development and regeneration of the zebrafish maxillary barbel: A novel study system for vertebrate tissue growth and repair. *PLoS One* 5(1):e8737.
39. Castillo D, et al. (2014) Induction of ectopic taste buds by SHH reveals the competency and plasticity of adult lingual epithelium. *Development* 141(15):2993–3002.
40. Barlow LA, Chien C-B, Northcutt RG (1996) Embryonic taste buds develop in the absence of innervation. *Development* 122(4):1103–1111.
41. Xu C-R, et al. (2011) Chromatin "prepattern" and histone modifiers in a fate choice for liver and pancreas. *Science* 332(6032):963–966.
42. Peng T, et al. (2013) Coordination of heart and lung co-development by a multipotent cardiopulmonary progenitor. *Nature* 500(7464):589–592.
43. Kague E, et al. (2012) Skeletogenic fate of zebrafish cranial and trunk neural crest. *PLoS One* 7(11):e47394.
44. Liu H-X, Komatsu Y, Mishina Y, Mistretta CM (2012) Neural crest contribution to lingual mesenchyme, epithelium and developing taste papillae and taste buds. *Dev Biol* 368(2):294–303.
45. Järvinen E, et al. (2006) Continuous tooth generation in mouse is induced by activated epithelial Wnt/β-catenin signaling. *Proc Natl Acad Sci USA* 103(49): 18627–18632.
46. Wang X-P, et al. (2009) Apc inhibition of Wnt signaling regulates supernumerary tooth formation during embryogenesis and throughout adulthood. *Development* 136(11):1939–1949.
47. Dassule HR, Lewis P, Bei M, Maas R, McMahon AP (2000) Sonic hedgehog regulates growth and morphogenesis of the tooth. *Development* 127(22):4775–4785.
48. Ohazama A, et al. (2009) Primary cilia regulate Shh activity in the control of molar tooth number. *Development* 136(6):897–903.
49. Kassai Y, et al. (2005) Regulation of mammalian tooth cusp patterning by ectodin. *Science* 309(5743):2067–2070.
50. Plikus MV, et al. (2005) Morphoregulation of teeth: Modulating the number, size, shape and differentiation by tuning Bmp activity. *Evol Dev* 7(5):440–457.
51. Wang X-P, et al. (2004) Follistatin regulates enamel patterning in mouse incisors by asymmetrically inhibiting BMP signaling and ameloblast differentiation. *Dev Cell* 7(5): 719–730.
52. Kawasaki K, et al. (2012) Bmp signalling in filiform tongue papillae development. *Arch Oral Biol* 57(6):805–813.
53. Zhou Y, Liu H-X, Mistretta CM (2006) Bone morphogenetic proteins and noggin: Inhibiting and inducing fungiform taste papilla development. *Dev Biol* 297(1):198–213.
54. Beites CL, et al. (2009) Follistatin modulates a BMP autoregulatory loop to control the size and patterning of sensory domains in the developing tongue. *Development* 136(13):2187–2197.
55. Davidson EH, Erwin DH (2006) Gene regulatory networks and the evolution of animal body plans. *Science* 311(5762):796–800.
56. Heanue TA, et al. (1999) Synergistic regulation of vertebrate muscle development by Dach2, Eya2, and Six1, homologs of genes required for *Drosophila* eye formation. *Genes Dev* 13(24):3231–3243.
57. Fujimura K, Okada N (2007) Development of the embryo, larva and early juvenile of Nile tilapia *Oreochromis niloticus* (Pisces: Cichlidae). Developmental staging system. *Dev Growth Differ* 49(4):301–324.
58. Su N, Ching V, Grushka M (2013) Taste disorders: A review. *J Can Dent Assoc* 79: d86.
59. Schneider CA, Rasband WS, Eliceiri KW (2012) NIH Image to ImageJ: 25 years of image analysis. *Nat Methods* 9(7):671–675.
60. Dingerkus G, Uhler LD (1977) Enzyme clearing of Alcian blue stained whole small vertebrates for demonstration of cartilage. *Stain Technol* 52(4):229–232.
61. Streelman JT, Albertson RC, Kocher TD (2003) Genome mapping of the orange blotch colour pattern in cichlid fishes. *Mol Ecol* 12(9):2465–2471.
62. Parnell NF, Streelman JT (2013) Genetic interactions controlling sex and color establish the potential for sexual conflict in Lake Malawi cichlid fishes. *Heredity (Edinb)* 110(3):239–246.
63. Streelman JT, Webb JF, Albertson RC, Kocher TD (2003) The cusp of evolution and development: a model of cichlid tooth shape diversity. *Evol Dev* 5(6):600–608.
64. Albertson RC, Kocher TD (2005) Genetic architecture sets limits on transgressive segregation in hybrid cichlid fishes. *Evolution* 59(3):686–690.

65. Albertson RC, Streelman JT, Kocher TD, Yelick PC (2005) Integration and evolution of the cichlid mandible: The molecular basis of alternate feeding strategies. *Proc Natl Acad Sci USA* 102(45):16287–16292.
66. Lee B-Y, et al. (2005) A second-generation genetic linkage map of tilapia (*Oreochromis* spp.). *Genetics* 170(1):237–244.
67. Broman KW, Sen S (2009) *A Guide to QTL Mapping with R/qtl* (Springer, New York), Vol 46.
68. Loh YHE, et al. (2008) Comparative analysis reveals signatures of differentiation amid genomic polymorphism in Lake Malawi cichlids. *Genome Biol* 9(7):R113.
69. Fraser GJ, Bloomquist RF, Streelman JT (2013) Common developmental pathways link tooth shape to regeneration. *Dev Biol* 377(2):399–414.
70. Wilkinson DG, Bhatt S, McMahon AP (1989) Expression pattern of the FGF-related proto-oncogene int-2 suggests multiple roles in fetal development. *Development* 105(1):131–136.